BIOCHEMISTRY
including biophysical chemistry & molecular biology

Article

pubs.acs.org/biochemistry

Comparison between the Aggregation of Human and Rodent Amyloid β-Proteins in GM1 Ganglioside Clusters

Hiroshi Ueno, Takahiro Yamaguchi, Saori Fukunaga, Yuki Okada, Yoshiaki Yano, Masaru Hoshino, and Katsumi Matsuzaki*

Graduate School of Pharmaceutical Sciences, Kyoto University, 46-29 Yoshida-Shimoadachi-cho, Sakyo-ku, Kyoto 606-8501, Japan

ABSTRACT: The abnormal deposition of amyloids by amyloid-β protein (Aβ) is a pathological hallmark of Alzheimer's disease (AD). Aged rodents rarely develop the characteristic lesions of the disease, which is different from the case in humans. Rodent Aβ (rAβ) differs from human Aβ (hAβ) only in the three substitutions of Arg to Gly, Tyr to Phe, and His to Arg at positions 5, 10, and 13, respectively. Understanding the reason why rodent Aβ does not form amyloids is important to revealing factors that cause the abnormal aggregation of Aβ under pathologic conditions. We have proposed that the binding of Aβ to membranes with ganglioside clusters plays an important role in the abnormal aggregation of Aβ. In this study, we compared hAβ and rAβ in terms of aggregation on neuronal cells, on raftlike model membranes, and in buffer. We found that rAβ formed amyloid fibrils similar to those of hAβ in buffer solution. In contrast, on cell membranes and raftlike membranes, hAβ formed toxic, mature amyloid fibrils, whereas rAβ produced less toxic protofibrils that were not stained by the amyloid-specific dye Congo red. Thus, our ganglioside cluster-mediated amyloidogenesis hypothesis explains the immunity of rodents from cerebral Aβ amyloid deposition, strengthening the importance of ganglioside clusters as a platform of abnormal Aβ deposition in the pathology of AD.

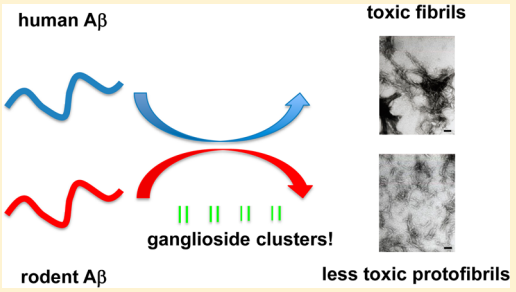

One of the pathological hallmarks of Alzheimer's disease (AD), a progressive neurodegenerative disease, is the deposition of senile plaques in the brain, the major component of which is fibrillar aggregates of amyloid-β protein (Aβ). Therefore, the conversion of the soluble, nontoxic Aβ monomer to aggregated toxic Aβ rich in β-sheet structures is considered a key step in the onset of AD.[1−3] There have been many controversies regarding the toxic species (oligomers or amyloid fibrils) and the mechanisms of toxicity (e.g., pore formation).[3,4] Recently, both oligomers and fibrils have been thought to be involved in the pathogenesis of AD.[4] Aged rodents, including rats, rarely develop the characteristic lesions of AD, which is different from the case in humans.[5] Rodent Aβ (rAβ) differs from human Aβ (hAβ) only in the three substitutions of Arg to Gly, Tyr to Phe, and His to Arg at positions 5, 10, and 13, respectively (Figure 1). Understanding why rAβ does not form amyloids is important for revealing factors that cause the abnormal aggregation of Aβ under pathologic conditions.

Metal ions have been shown to accelerate the aggregation of hAβ.[6] Bush et al. reported that submicromolar concentrations of Zn^{2+} ions induced amyloid formation by hAβ, whereas rAβ was immune to this effect.[7] Cu^{2+} ions also induce limited aggregation by hAβ, but not by rAβ, which is enhanced by slightly acidic conditions.[8] The His^{13} residue present only in hAβ is crucial for these interactions.[8,9] The metals also enhance the disruption of phospholipid bilayers by Aβ.[10]

Not only the binding of metal ions by Aβ but also the binding of Aβ to cell membranes, especially to ganglioside-containing ones, has been reported to play an important role in the aggregation of Aβ.[11−14] On the basis of the discovery of a monosialoganglioside GM1-bound form of Aβ in the brains of AD patients,[15] we have proposed the following scenario for the membrane-catalyzed abnormal aggregation of Aβ. Soluble Aβ with an unordered structure specifically binds to lipid raft membranes containing GM1 clusters, the formation of which is induced by cholesterol.[16] The membrane-bound Aβ changes its conformation from a random coil to an α-helix-rich structure at a lower protein density. Above a threshold Aβ/GM1 value, the helical form is in equilibrium with a β-sheet-rich conformation composed of approximately 15 Aβ molecules. When the Aβ/GM1 ratio exceeds a second critical value, the β-sheet form is converted to a second β-sheet-rich species that can serve as a seed for the formation of amyloid fibrils.[17] The fibrils are more toxic than those formed in aqueous solution[18] and may have antiparallel β-sheets.[19]

In this paper, we compare hAβ and rAβ in terms of aggregation on neuronal cells, on raftlike model membranes, and in buffer. We found that rAβ formed amyloid fibrils similar to those of hAβ in buffer solution. In contrast, on cell membranes and raftlike membranes, hAβ formed toxic, mature amyloid fibrils whereas rAβ produced less toxic protofibrils that were not stained by the amyloid-specific dye Congo red. The importance of GM1 clusters in facilitating Aβ aggregation in the brain will be discussed.

Received: October 1, 2014
Revised: November 14, 2014
Published: November 14, 2014

   dx.doi.org/10.1021/bi501239q | *Biochemistry* 2014, 53, 7523−7530

hAβ-(1–40) : DAEFRHDSGY[10]EVHHQKLVFF[20]AEDVGSNKGA[30]IIGLMVGGVV[40]

rAβ-(1–40) : DAEFGHDSGF[10]EVRHQKLVFF[20]AEDVGSNKGA[30]IIGLMVGGVV[40]

Figure 1. Amino acid sequences of hAβ and rAβ. Substitutions are highlighted.

MATERIALS AND METHODS

Aβs. hAβ-(1−40) and rAβ-(1−40) were produced as ubiquitin extensions[20] and purified as described in detail elsewhere.[21] The purity (>95%) and identity of the protein were confirmed by analytical reverse phase high-performance liquid chromatography (HPLC) and electrospray ionization mass spectroscopy. The protein was dissolved in 0.02% ammonia on ice, and any large aggregates that may have acted as a seed for aggregation were removed by ultracentrifugation in 500 μL polyallomer tubes at 540000g and 4 °C for 3 h. The protein concentration of the supernatant was determined in triplicate by the Micro BCA protein assay (Pierce, Rockford, IL). The supernatant was collected and stored at −80 °C prior to being used. Just before the experiment, the stock solution was mixed with an equal volume of double-concentrated PBS [16.0 g/L NaCl, 0.40 g/L KCl, 2.3 g/L Na_2HPO_4, and 0.4 g/L KH_2PO_4 (pH 7.4)]. Aβs assumed a monomeric state under these conditions.[22]

Small Unilamellar Vesicles (SUVs). GM1 from bovine brain was purchased from Larodan (Malmö, Sweden). Cholesterol and *N*-acyl-D-sphingosine-1-phosphocholine from bovine brain (SM) were obtained from Sigma (St. Louis, MO). GM1/cholesterol/sphingomyelin (1/1/1) SUVs were prepared in PBS as described previously.[17] The vesicles have been characterized in terms of size and lamellarity.[23] The concentration of vesicles was determined on the basis of the concentration of GM1, which was determined at least in triplicate by the resorcinol−hydrochloric acid method,[24] because the lipid composition of vesicle preparations was very close to the expected value, within a margin of error of 10%.[23]

Cell Culture. Human SH-SY5Y neuroblastoma cells were obtained from ECACC and cultured in D-MEM/F-12 containing 10% FBS, 100 units/mL penicillin, and 0.1 mg/mL streptomycin. After being plated at a density of 9000−10000 cells/well onto a coverglass base, optical bottom 96-well microplate (Nunc, Roskilde, Denmark), the cells were incubated for more than 24 h at 37 °C with 5% CO_2 to allow cell attachment.[25]

Staining of Live Cells and Amyloid Fibrils. Cells were incubated with freshly prepared hAβ and rAβ (50 μM) in medium at 37 °C with 5% CO_2. The live cells and amyloid fibrils were stained with 0.1 μM calcein AM (excitation at 488 nm; emission at BP 500−550 nm) and 20 μM Congo red (excitation at 561 nm; emission at BP 575−615 nm), respectively, for 30 min at room temperature.[25] Before and after the staining step, the cells were rinsed twice with PBS containing 0.01% calcium and 0.01% magnesium (PBS+). The cells were visualized using the CFI Plan Apochromat VC 60× WI/1.20 objective of a C1si confocal laser scanning microscope (Nikon, Tokyo, Japan).

Thioflavin T (Th-T) Assay. hAβ and rAβ (50 μM) were incubated in PBS or with raftlike GM1/cholesterol/SM (1/1/1) SUVs (50 μM GM1) at 37 °C. Aggregation of Aβs was monitored by the Th-T assay. The sample (final Aβ concentration of 0.5 μM) was added to a 5 μM Th-T solution in 50 mM glycine buffer (pH 8.5). Fluorescence at 490 nm was measured at an excitation wavelength of 446 nm at 25 °C.[26,27] The blank fluorescence (buffer or SUV suspension) was subtracted.

Transmission Electron Microscopy (TEM). TEM experiments were conducted by the Ultrastructure Research Institute of Hanaichi Co. Ltd. (Okazaki, Japan). Samples were spread on carbon-coated grids, negatively stained with uranyl acetate, and examined under a JEOL JEM-2000EX electron microscope with an acceleration voltage of 100 kV.

Congo Red Binding. Aggregated Aβs were also stained with Congo red and observed by a Nikon total internal reflection fluorescence microscope (TIRFM), as described elsewhere.[25]

Cytotoxicity. hAβ and rAβ (50 μM) were incubated with raftlike GM1/cholesterol/SM (1/1/1) SUVs (50 μM GM1) at 37 °C for 2 days. The incubated Aβ sample containing SUVs was mixed with an equal volume of medium (final concentration of 25 μM), and a 100 μL portion of the solution was applied to each well and incubated for 24 h at 37 °C with 5% CO_2. Fifty microliters of 3 μM ethidium homodimer-1 in PBS was added to each well (final concentration of 1 μM) without removing the sample solution.[22] Ethidium homodimer-1 enters cells with damaged membranes and produces fluorescence in dead cells. Fluorescence was measured on a Wallac Envision instrument (PerkinElmer, Waltham, MA). Linearity between the number of dead cells and fluorescence intensity of ethidium homodimer-1 (excitation at 531 nm; emission at 620 nm) was confirmed. The fluorescence intensity of cells treated with only SUVs was defined as a positive control (100% viability), and the fluorescence intensity of those treated with 70% (v/v) methanol for 30 min was defined as a negative control (0% viability). The statistical analysis was performed using one-way analysis of variance (n = 6).

Binding of Aβ to Raftlike SUVs. hAβ and rAβ (50 μM) were mixed with raftlike SUVs and equilibrated for 5 min at 37 °C. The free Aβ monomers and SUV-bound Aβ were separated by ultracentrifugation at 200000g and 37 °C for 3 h. The peptide concentration in the supernatant was determined by analytical HPLC, which was performed using a COSMOSIL Packed Column $5C_{18}$-AR-II [4.6 mm (inside diameter) × 150 mm] (Nacalai Tesque, Kyoto, Japan) eluted with a linear gradient of CH_3CN (from 25 to 50% over 30 min) in 0.1% aqueous trifluoroacetic acid at a flow rate of 1 mL/min.[17] The protein was detected by measuring the UV absorbance at 220 nm.

Circular Dichroism (CD) Spectra. hAβ and rAβ (15 μM) were mixed with various concentrations of raftlike SUVs. CD spectra were recorded on a Jasco (Hachioji, Japan) J-820 apparatus at 37 °C, using a 1 mm path length quartz cell to minimize the absorbance due to buffer components. Eight scans (scan rate of 20 nm/min; wavelength range of 195−250 nm) were averaged for each sample, and the blank spectra (buffer or SUV suspension) were subtracted.[17]

Fourier Transform Infrared (FTIR) Spectra. Amyloid fibrils were collected by centrifugation (20000g for 10 min) and washed with water five times. Protofibrils formed by rAβ in the

dx.doi.org/10.1021/bi501239q | *Biochemistry* 2014, 53, 7523−7530

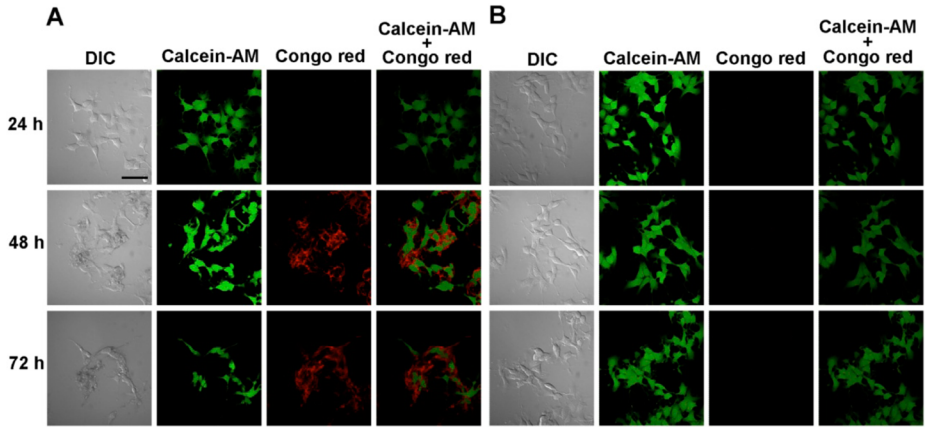

Figure 2. Fibril formation by (A) hAβ and (B) rAβ on neuronal cell membranes. SH-SY5Y cells were incubated with each Aβ (50 μM) at 37 °C for 24, 48, or 72 h. Live cells and Aβ fibrils on cell membranes were simultaneously visualized with calcein AM and Congo red, respectively. DIC, calcein AM, Congo red, and merged images are shown from left to right, respectively. The scale bar is 50 μm.

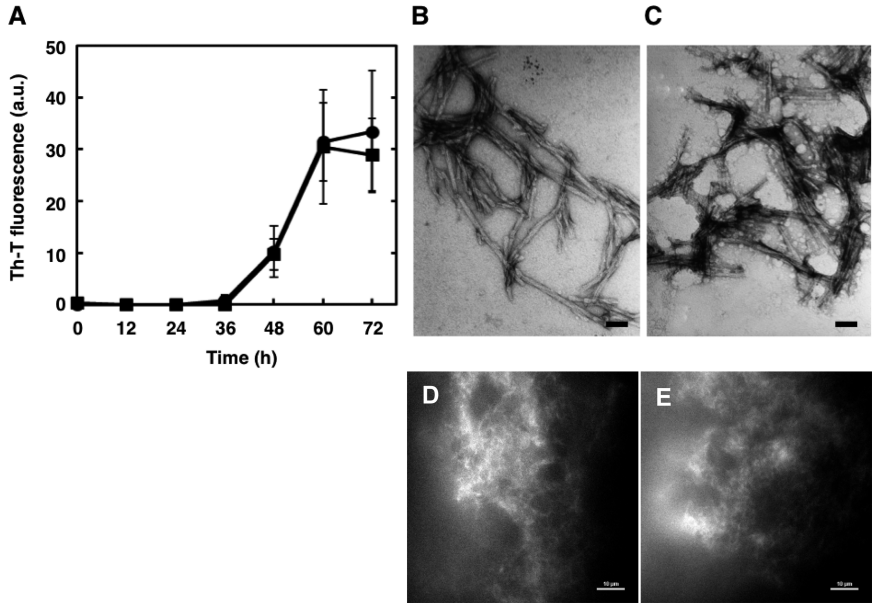

Figure 3. Formation of fibrils by Aβs in PBS. hAβ (●) and rAβ (■) were incubated at 37 °C without agitation (50 μM Aβ). (A) Fibril formation was monitored by the Th-T assay (mean ± standard error; n = 2). The morphology of (B) hAβ fibrils and (C) rAβ fibrils was observed by TEM. The scale bars are 50 nm. (D) hAβ fibrils and (E) rAβ fibrils were also observed by a TIRFM after Congo red staining. The scale bars are 10 μm.

presence of raftlike membranes were precipitated with vesicles by ultracentrifugation (200000g and 37 °C for 3 h). Dry films of aggregates were prepared by spreading the pellets on a germanium attenuated total reflection (ATR) plate (80 mm × 10 mm × 4 mm) under a stream of nitrogen gas. The residual water was removed on P_2O_5 under vacuum overnight. Trifluoroacetic acid originating from Aβ, which gives absorption in the amide I region,[28] was completely eliminated by this procedure.[19] FTIR-ATR measurements were taken on a Bruker (Ettringen, Germany) TENSOR 27 spectrometer equipped with a Hg−Cd−Te detector and a PIKE horizontal ATR attachment. The total reflection number was 10 on the film side. The spectra were measured at a resolution of 2 cm^{-1} and an angle of incidence of 45° and derived from 256 co-added interferograms with the Happ−Genzel apodization function. Subtraction of the gently sloping water vapor was conducted to improve the background prior to frequency measurement. For ATR correction, refractive indexes of 4.003 and 1.7 were used for germanium and protein, respectively. In the case of rAβ protofibrils, spectra of SUVs were subtracted.

RESULTS

Formation of Fibrils by Aβs on Living Cell Membranes. The formation of amyloid fibrils on living cell membranes was visualized using the amyloid-staining dye Congo red and calcein AM.[25] Calcein AM is a membrane-permeable dye that is cleaved by intracellular esterases to produce the membrane-impermeable fluorophore calcein in viable cells. The cell viability was calculated from the number of calcein-positive cells divided by the total number of cells (100−200). When cells were incubated with 50 μM hAβ (Figure 2A), the cell viability remained 98% at 24 h. The formation of Congo red-positive amyloid fibrils on cell membranes was detected at 48 h, and the cells started to die (viability of 84%). After 72 h, significant cell death was observed (viability of 70%) and the cell debris was covered with substantial amounts of amyloid fibrils. In contrast, when cells were incubated with 50

dx.doi.org/10.1021/bi501239q | Biochemistry 2014, 53, 7523−7530

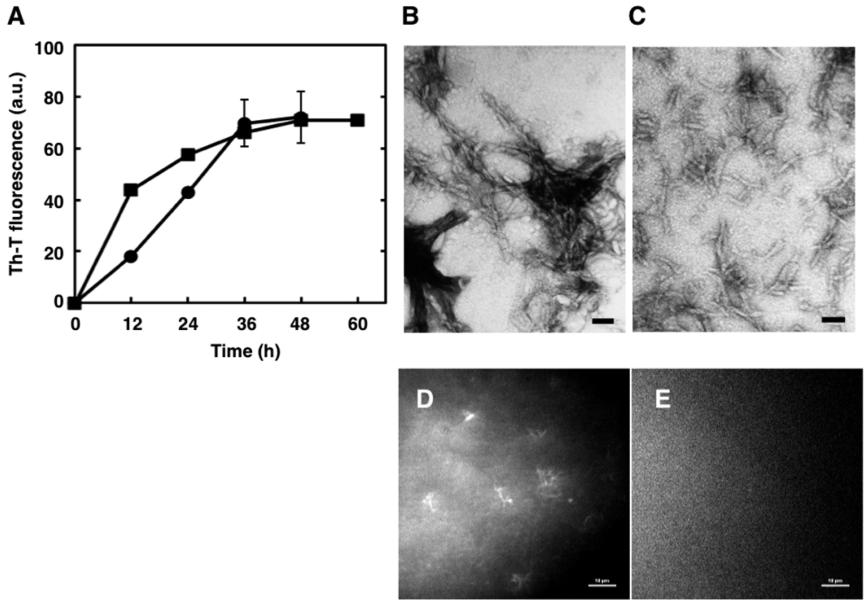

Figure 4. Formation of fibrils by Aβs in the presence of raftlike SUVs. hAβ (●) and rAβ (■) were incubated with raftlike GM1/cholesterol/SM (1/1/1) SUVs at 37 °C without agitation (50 μM Aβ and GM1/Aβ ratio of 1). (A) Fibril formation was monitored by the Th-T assay (mean ± standard error; n = 2). The morphology of (B) hAβ fibrils and (C) rAβ fibrils was observed by TEM. The scale bars are 50 nm. (D) hAβ fibrils and (E) rAβ fibrils were also observed by a TIRFM after Congo red staining. The scale bars are 10 μm.

μM rAβ, neither significant Congo red-positive amyloid fibrils nor cell death was observed even after 72 h (Figure 2B). The cell viability was 99, 96, and 92% at 24, 48, and 72 h, respectively.

Formation of Fibrils by Aβs in PBS. Aggregation of Aβs in PBS was monitored as an increase in Th-T fluorescence intensity (Figure 3A). Both hAβ and rAβ aggregated after a long lag time (1.5 days), and the aggregation kinetics were similar. The morphology of the fibrils was observed by TEM (Figure 3B,C). Both hAβ and rAβ formed similar typical amyloid fibrils with widths of 7.9 ± 0.6 and 8.0 ± 0.4 nm, respectively. The two types of fibrils were observed by a TIRFM after Congo red staining (Figure 3D,E). Both were stained by the amyloid-specific agent.

Formation of Fibrils by Aβs in the Presence of Raftlike SUVs. We performed similar experiments in the presence of raftlike GM1/cholesterol/SM (1/1/1) SUVs, which mimic lipid raft microdomains on cell membranes. Both types of Aβ aggregated without a lag time, but the aggregation kinetics were different; rAβ aggregated faster than hAβ did (Figure 4A). TEM images revealed that the morphology of the aggregates was also different; hAβ formed mature amyloid fibrils with a width of 12.9 ± 0.7 nm (Figure 4B) that are thicker than the fibrils formed in buffer (Figure 3B), whereas rAβ formed short protofibrillar aggregates with a width of 8.1 ± 0.5 nm (Figure 4C). The latter aggregates could not be spun down even at 20000g, the conditions under which the hAβ fibrils could be centrifuged.[18] The two types of aggregates were observed by a TIRFM after Congo red staining (Figure 4D,E). Only hAβ fibrils were stained by the amyloid-specific agent. These results indicate that the formation of fibrils by Aβs was significantly affected by the presence of raftlike SUVs; interestingly, rAβ did not form mature amyloid fibrils.

Toxicity of Fibrils against Cells. We have previously shown that hAβ fibrils generated in buffer were nontoxic after a 24 h incubation with 25 μM aggregates.[19] To characterize hAβ fibrils and rAβ protofibrils formed in the presence of raftlike SUVs, we examined the toxicity of these aggregates against neuronal cells under the same conditions. The toxicity of hAβ fibrils and rAβ protofibrils was determined by using ethidium homodimer-1 (Figure 5).[22] The rAβ protofibrils were almost nontoxic. In contrast, cell viability in the presence of hAβ fibrils was significantly lower than that of the rAβ sample.

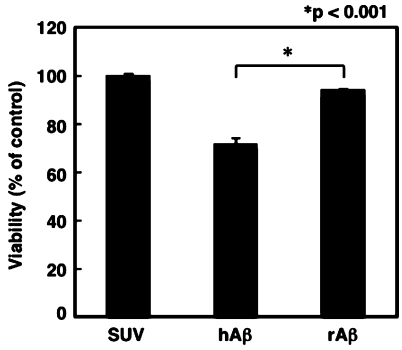

Figure 5. Cytotoxicity of preformed Aβ fibrils. The viability of SH-SY5Y cells in the presence of 25 μM hAβ fibrils and rAβ protofibrils was estimated with the fluorescence intensity of ethidium homodimer-1 after a 24 h incubation at 37 °C (mean ± standard error; n = 6; *p < 0.001 between hAβ and rAβ). The sample without fibrils (SUVs only) was used as a control for 100% viability.

Binding of Aβs to Raftlike SUVs. The binding of Aβs to raftlike SUVs was directly assessed by a combination of ultracentrifugation and analytical HPLC.[17] The amount of membrane-bound Aβ per GM1 in the outer leaflet of liposomes, x (moles per mole), was plotted as a function of the free Aβ concentration, C_f (Figure 6). The binding equilibrium could be phenomenologically expressed by Langmuir's equation:[17]

$$x = \frac{x_{max} K C_f}{1 + K C_f} \quad (1)$$

dx.doi.org/10.1021/bi501239q | Biochemistry 2014, 53, 7523−7530

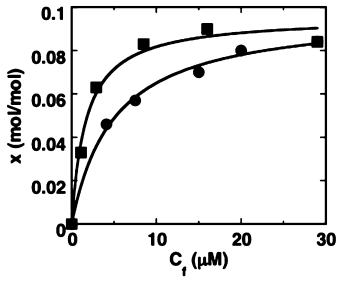

Figure 6. Binding isotherm of Aβs at 37 °C. The binding of hAβ (●) and rAβ (■) to GM1/cholesterol/SM (1/1/1) SUVs was directly assessed by ultracentrifugation and analytical HPLC. The amount of SUV-bound Aβ per GM1 in the outer leaflet, x, is plotted as a function of the free Aβ concentration, C_f. The curves are best fits to Langmuir's equation. The fitting parameters are summarized in Table 1.

The maximal x values (x_{max}) and the binding constants (K) are summarized in Table 1. The x_{max} values were similar between

Table 1. Parameters for the Binding of Aβs to GM1/Cholesterol/SM (1/1/1) SUVs at 37 °C

Aβ	x_{max} [Aβ/GM1 (mol/mol)]	K ($\times 10^5$ M^{-1})
hAβ-(1−40)	0.0976 ± 0.0034	1.99 ± 0.25
rAβ-(1−40)	0.0956 ± 0.0042	5.88 ± 1.19

hAβ and rAβ, indicating that both types of Aβ bind to the same binding site, i.e., the GM1 cluster. On the other hand, rAβ exhibited a binding affinity 3-fold higher than that of hAβ.

CD. The secondary structures of Aβs in the presence and absence of SUVs were estimated from CD spectra at 37 °C. The CD spectra of membrane-bound Aβ were obtained by subtracting the contributions from free Aβ.[17] The fraction of free Aβ, f, was calculated using the following equations:

$$C = C_{tot} f \tag{2}$$

$$x = \frac{2(1-f)}{[GM1]/C_{tot}} = \frac{x_{max} K C_f}{1 + K C_f} \tag{3}$$

where C_{tot} represents the total concentration of Aβ.

The mean residue molar ellipticity of membrane-bound Aβ ($[\theta]_{bound}$) was calculated as follows:

$$[\theta]_{bound} = \frac{[\theta]_{obs} - f[\theta]_{free}}{1 - f} \tag{4}$$

The mean residue molar ellipticities of Aβ determined in the presence and absence of SUVs are denoted by $[\theta]_{obs}$ and $[\theta]_{free}$, respectively.

Although hAβ and rAβ formed different types of aggregates in raftlike membranes, both Aβs exhibited similar structural changes from α-helix-rich structures to β-sheet-rich structures as the x value increased (Figure 7A,B). However, the α-helix-rich structures and β-sheet-rich structures were not identical beween hAβ and rAβ. At lower x values, rAβ exhibited a mean residue molar ellipticity around 222 nm less negative than that of hAβ, indicating that rAβ contained less α-helical structure than hAβ did (Figure 7C). At higher x values, rAβ exhibited a minimum at a wavelength longer than that of hAβ, indicating that rAβ assumed a β-structure different from that of hAβ (Figure 7C).

FTIR. The secondary structures of Aβ aggregates formed in the presence of raftlike membranes were estimated by FTIR. Mature fibrils formed by hAβ and protofibrils formed by rAβ exhibited major bands at 1630 and 1626 cm^{-1}, respectively, concomitant with minor absorptions at ∼1695 cm^{-1} (Figure 8), suggesting the possible presence of some antiparallel β-sheets,[29−31] although this band may not be unique to antiparallel β-sheets.[32]

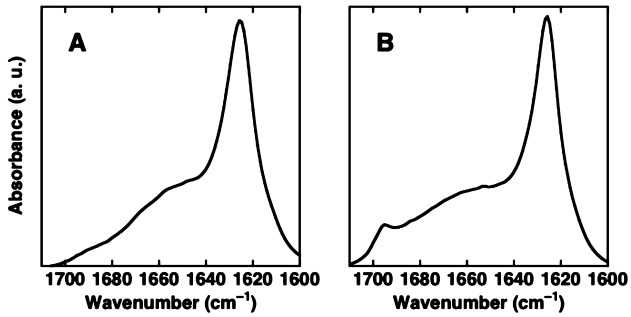

Figure 8. FTIR spectra of (A) hAβ fibrils and (B) rAβ protofibrils formed in the presence of raftlike membranes.

DISCUSSION

Both types of Aβs have been less extensively compared, especially in terms of membrane interaction, although the following facts suggest that the primary structure of Aβ itself determines whether the animal suffers from AD-like pathology. First, not only humans but also aged lower primates and other mammals, such as dogs, form cerebral Aβ amyloid deposits.[33]

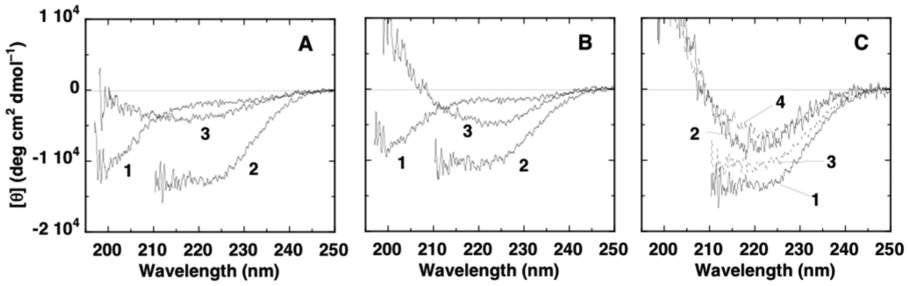

Figure 7. CD spectra of Aβs. Observed CD spectra of 15 μM (A) hAβ and (B) rAβ in the absence or presence of raftlike GM1/cholesterol/SM (1/1/1) SUVs were measured at 37 °C. The overall Aβ/GM1 ratios (x values) are (A) 0, 0.0083 (0.0156), and 0.1 (0.0652) and (B) 0, 0.0083 (0.0163), and 0.05 (0.0696) for traces 1−3, respectively. (C) Comparison of secondary structures of membrane-bound hAβ (traces 1 and 2) and rAβ (traces 3 and 4) at similar x values. Membrane-bound spectra were calculated from panels A and B of Figure 8 by the use of binding isotherms. The x values are 0.0156, 0.0652, 0.0163, and 0.0696 for traces 1−4, respectively.

dx.doi.org/10.1021/bi501239q | Biochemistry 2014, 53, 7523−7530

The Aβs of these plaque-developing animals have an amino acid sequence identical to that of hAβ, and that of the plaque-free mouse is the same as that of rAβ. Second, transgenic mice producing excess hAβ[34] and the exogeneous administration of hAβ in rodents[35] have been widely used as animal models for AD. Interestingly, a similar human versus rat issue is also present for the amyloidogenic amylin peptide related to type II diabetes.[36,37]

In PBS, both hAβ and rAβ aggregated with similar kinetics and formed mature amyloid fibrils with similar morphology and Congo red staining (Figure 3), indicating that the three amino acid substitutions essentially do not affect amyloidogenesity, at least in the absence of metals. In contrast, hAβ and rAβ behaved differently in the presence of raftlike membranes. The binding affinity of Aβ is proportional to the slope of the isotherm close to the origin, where the protein assumed the helical form. The rAβ more strongly bound to the bilayers than hAβ did (Figure 6), despite the fact that rAβ was less helical (Figure 7C). This can be explained as follows. The interaction of hAβ with GM1 micelles was reported to be localized to its N-terminal region, particularly residues His^{13}–Leu^{17}, which became more helical when bound.[38] The α-helical conformations of hAβ have also been determined in sodium dodecyl sulfate[39−41] and lyso-GM1 micelles[42] by nuclear magnetic resonance (NMR). The protein had two helical regions, and the first one (residues 15−24,[39,41] 10−24,[40] or 14−24[42]) contained or was adjacent to the His^{13} residue. The helical wheel representation of residues 10−24 (Figure 9) suggests

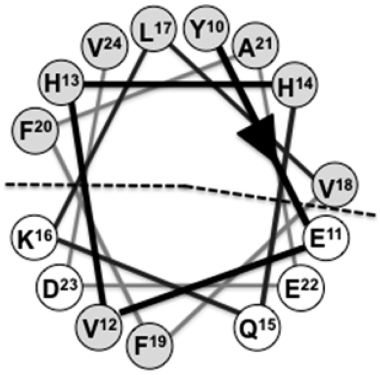

Figure 9. Helical wheel representation of hAβ-(10−24). Hydrophobic residues are highlighted in gray, assuming that the His residues are deprotonated. The dashed line denotes a hydrophilic−hydrophobic interface.

that this region, especially residues 13−24, potentially forms an amphipathic helix with the His^{13} residue embedded in the hydrophobic face. The introduction of a positive charge by the His-to-Arg substitution at this site is expected to destabilize the amphipathic helix, thus decreasing the helicity. However, the increased net charge of this membrane-binding region will strengthen the binding of the protein to the negatively charged membranes. Although an NMR study suggested a possible interaction between Arg^5 of hAβ and GM1,[38] this residue appears not to be significantly involved in the binding: the N-termini of both Aβs have the same net charge.

rAβ exhibited neither amyloid formation on neuronal cells nor cytotoxicity (Figure 2). The fact that the protein formed Th-T-positive but Congo red-negative protofibrils (Figure 4) without cytotoxicity (Figure 5) in the presence of raftlike liposomes suggests that rAβ also formed nontoxic protofibrils on neuronal cells that could not be detected with Congo red. Th-T could not be used for the detection of protein aggregates on living cells because of strong background staining.[43] Both Congo red and Th-T are considered to bind to a side-chain groove running roughly parallel to the fibril axis, although the molecular mechanisms by which these dyes recognize various types of amyloid fibrils are not well understood. The fact that Congo red recognizes a longer order may explain the failure of the dye to stain protofibrils by rAβ. The negatively charged sulfate groups of Congo red bind to two positively charged residues separated by a distance of 19 Å,[44] whereas the head-to-tail length of Th-T is ∼15 Å.[45] Furthermore, Th-T also binds to hydrophobic pockets in globular proteins.[45]

FTIR spectra suggested that both hAβ and rAβ aggregates, at least partly, may contain some antiparallel β-sheet structures. For a detailed discussion, see ref 19. Although the minor band at ∼1695 cm^{-1} was obscure for hAβ, preliminary experiments using chemical cross-linking, isotope-edited FTIR, and solid-state NMR support this conclusion. The presence of antiparallel β-sheets has been reported to correlate closely with the cytotoxicity of various amyloid fibrils and soluble oligomers.[46,47] However, the absence of cytotoxicity for rAβ protofibrils (Figure 5) indicates that this emerging rule of thumb does not always hold.

Any aggregation mechanisms leading to AD pathology should address the following questions: (1) Does the mechanism explain major risk factors for AD, such as aging or the apo E4 allele?[48] (2) Does the mechanism explain the region-dependent deposition of Aβ in the AD brain? (3) Was the hypothesis verified *in vivo*?

With regard to question 1, the amount of cholesterol, which facilitates GM1 clustering,[16] in the exofacial leaflets of the synaptic plasma membrane increases in aged[49] as well as apolipoprotein E4-knock-in[50] mice. Age-dependent GM1 clustering occurs at presynaptic neuritic terminals in mouse brains,[51] at which Aβ deposition likely starts.[52,53] With regard to to question 2, the region-dependent deposition of Aβ could be explained by the local ganglioside species for several familial AD-related variant Aβs.[54,55] Several lines of evidence answer question 3. Antibody 4396C raised against GM1-bound Aβ bound to membrane fibrils and also immunostained the cerebral cortex of AD brains, but not control brains.[56] Furthermore, the peripheral administration of cell-penetrating peptide-modified Fab fragments of 4396C to transgenic mice expressing a mutant APP gene substantially suppressed Aβ deposition in the brain.[57]

The study presented here reveals that AD-developing hAβ formed toxic, mature amyloid fibrils, whereas AD-immune rAβ produced less toxic protofibrils on membranes containing GM1 clusters. We conclude that, in addition to the metal-catalyzed amyloid formation mechanism, our GM1 cluster-mediated amyloidogenesis hypothesis also explains the observation that aged rodents rarely develop the characteristic lesions of AD, strengthening the importance of ganglioside clusters as a platform of abnormal Aβ deposition in the pathology of AD.

AUTHOR INFORMATION

Corresponding Author

*Phone: +81 75-753-4521. Fax: +81 75-753-4578. E-mail: mkatsumi@pharm.kyoto-u.ac.jp.

Funding

This work was supported in part by The Research Funding for Longevity Sciences (22-14 and 25-19) from the National Center for Geriatrics and Gerontology (NCGG) of Japan.

Notes

The authors declare no competing financial interest.

REFERENCES

(1) Hardy, J., and Selkoe, D. J. (2002) The amyloid hypothesis of Alzheimer's disease: Progress and problems on the road to therapeutics. *Science 297*, 353−356.

(2) Walsh, D. M., and Selkoe, D. J. (2004) Deciphering the molecular basis of memory failure in Alzheimer's disease. *Neuron 44*, 181−193.

(3) Masters, C. L., and Selkoe, D. J. (2012) Biochemistry of amyloid β-protein and amyloid deposits in Alzheimer disease. *Cold Spring Harbor Perspect. Med. 2*, a006262.

(4) Selkoe, D. J. (2011) Resolving controversies on the path to Alzheimer's therapeutics. *Nat. Med. 17*, 1060−1065.

(5) Selkoe, D. J. (1989) Biochemistry of altered brain proteins in Alzheimer's disease. *Annu. Rev. Neurosci. 12*, 463−490.

(6) Bush, A. I. (2003) The metallobiology of Alzheimer's disease. *Trends Neurosci. 26*, 207−214.

(7) Bush, A. I., Pettingell, W. H., Multhaup, G., d Paradis, M., Vonsattel, J. P., Gusella, J. F., Beyreuther, K., Masters, C. L., and Tanzi, R. E. (1994) Rapid induction of Alzheimer Aβ amyloid formation by zinc. *Science 265*, 1464−1467.

(8) Atwood, C. S., Moir, R. D., Huang, X., Scarpa, R. C., Bacarra, N. M., Romano, D. M., Hartshorn, M. A., Tanzi, R. E., and Bush, A. I. (1998) Dramatic aggregation of Alzheimer Aβ by Cu(II) is induced by conditions representing physiological acidosis. *J. Biol. Chem. 273*, 12817−12826.

(9) Liu, S. T., Howlett, G., and Barrow, C. J. (1999) Histidine-13 is a crucial residue in the zinc ion-induced aggregation of the Aβ peptide of Alzheimer's disease. *Biochemistry 38*, 9373−9378.

(10) Lau, T.-L., Ambroggio, E. E., Tew, D. J., Cappi, R., Masters, C. L., Fidelio, G. D., Barnham, K. J., and Separovic, F. (2006) Amyloid-β peptide disruption of lipid membranes and the effect of metal ions. *J. Mol. Biol. 356*, 759−770.

(11) Matsuzaki, K. (2007) Physicochemical interactions of amyloid β-peptide with lipid bilayers. *Biochim. Biophys. Acta 1768*, 1935−1942.

(12) Matsuzaki, K., Kato, K., and Yanagisawa, K. (2010) Aβ polymerization through interaction with membrane gangliosides. *Biochim. Biophys. Acta 1801*, 868−877.

(13) Matsuzaki, K. (2011) Formation of toxic amyloid fibrils by amyloid β-protein on ganglioside clusters. *International Journal of Alzheimer's Research 2011*, ID 956104.

(14) Matsuzaki, K. (2014) How do membranes initiate Alzheimer's disease? Formation of toxic amyloid fibrils by the amyloid β-protein on ganglioside clusters. *Acc. Chem. Res. 47*, 2397−2404.

(15) Yanagisawa, K., Odaka, A., Suzuki, N., and Ihara, Y. (1995) GM1 ganglioside-bound amyloid β-protein (Aβ): A possible form of preamyloid in Alzheimer's disease. *Nat. Med. 1*, 1062−1066.

(16) Kakio, A., Nishimoto, S., Yanagisawa, K., Kozutsumi, Y., and Matsuzaki, K. (2001) Cholesterol-dependent formation of GM1 ganglioside-bound amyloid β-protein, an endogenous seed for Alzheimer amyloid. *J. Biol. Chem. 276*, 24985−24990.

(17) Ikeda, K., Yamaguchi, T., Fukunaga, S., Hoshino, M., and Matsuzaki, K. (2011) Mechanism of amyloid β-protein aggregation mediated by GM1 ganglioside clusters. *Biochemistry 50*, 6433−6440.

(18) Okada, T., Ikeda, K., Wakabayashi, M., Ogawa, M., and Matsuzaki, K. (2008) Formation of toxic Aβ (1−40) fibrils on GM1 ganglioside-containing membranes mimicking lipid rafts: Polymorphisms in Aβ (1−40) fibrils. *J. Mol. Biol. 382*, 1066−1074.

(19) Fukunaga, S., Ueno, H., Yamaguchi, T., Yano, Y., Hoshino, M., and Matsuzaki, K. (2012) GM1 cluster mediates formation of toxic Aβ fibrils by providing hydrophobic environments. *Biochemistry 51*, 8125−8131.

(20) Lee, E. K., Hwang, J. H., Shin, D. Y., Kim, D. I., and Yoo, Y. J. (2005) Production of recombinant amyloid-β peptide 42 as an ubiquitin extension. *Protein Expression Purif. 40*, 183−189.

(21) Yamaguchi, T., Yagi, H., Goto, Y., Matsuzaki, K., and Hoshino, M. (2010) A disulfide-linked amyloid-β peptide dimer forms a protofibril-like oligomer through a distinct pathway from amyloid fibril formation. *Biochemistry 49*, 7100−7107.

(22) Okada, T., Wakabayashi, M., Ikeda, K., and Matsuzaki, K. (2007) Formation of toxic fibrils of Alzheimer's amyloid β-protein-(1−40) by monosialoganglioside GM1, a neuronal membrane component. *J. Mol. Biol. 371*, 481−489.

(23) Yamamoto, N., Matsuzaki, K., and Yanagisawa, K. (2005) Cross-seeding of wild-type and hereditary variant type amyloid β-proteins in the presence of gangliosides. *J. Neurochem. 95*, 1167−1176.

(24) Svennerholm, L. (1957) Quantitative estimation of sialic acids. II. A colorimetric resorcinol-hydrochloric acid method. *Biochim. Biophys. Acta 24*, 604−611.

(25) Ogawa, M., Tsukuda, M., Yamaguchi, T., Ikeda, K., Okada, T., Yano, Y., Hoshino, M., and Matsuzaki, K. (2011) Ganglioside-mediated aggregation of amyloid β-proteins (Aβ): Comparison between Aβ-(1−42) and Aβ-(1−40). *J. Neurochem. 116*, 851−857.

(26) LeVine, H., III (1993) Thioflavin T interaction with synthetic Alzheimer's disease β-amyloid peptides: Detection of amyloid aggregation in solution. *Protein Sci. 2*, 404−410.

(27) Naiki, H., and Gejyo, F. (1999) Kinetic analysis of amyloid fibril formation. *Methods Enzymol. 309*, 305−318.

(28) Surewicz, W. K., and Mantsch, H. H. (1989) The conformation of dynorphin A-(1−13) in aqueous solution as studied by Fourier transform infrared spectroscopy. *J. Mol. Struct. 214*, 143−147.

(29) Miyazawa, T. (1960) Perturbation treatment of the characteristic vibrations of polypeptide chains in various configurations. *J. Chem. Phys. 32*, 1647−1652.

(30) Miyazawa, T., and Blout, E. R. (1961) The infrared spectra of polypeptides in various conformations: Amide I and II bands. *J. Am. Chem. Soc. 83*, 712−719.

(31) Jackson, M., and Mantsch, H. H. (1995) The use and misuse of FTIR spectroscopy in the determination of protein structure. *Crit. Rev. Biochem. Mol. Biol. 30*, 95−120.

(32) Khurana, R., and Fink, A. L. (2000) Do parallel β-helix proteins have a unique Fourier transform infrared spectrum? *Biophys. J. 78*, 994−1000.

(33) Selkoe, D. J., Bell, D. S., Podlisny, M. B., Price, D. L., and Cork, L. C. (1987) Conservation of brain amyloid proteins in aged mammals and humans with Alzheimer's disease. *Science 235*, 873−877.

(34) Philipson, O., Lord, A., Gumucio, A., O'Callaghan, P., Lannfelt, L., and Nilsson, L. N. (2010) Animal models of amyloid-β-related pathologies in Alzheimer's disease. *FEBS J. 277*, 1389−1409.

(35) Chambon, C., Wegener, N., Gravius, A., and Danysz, W. (2011) Behavioural and cellular effects of exogenous amyloid-β peptides in rodents. *Behav. Brain Res. 225*, 623−641.

(36) Nanga, R. P., Brender, J. R., Xu, J., Hartman, K., Subramanian, V., and Ramamoorthy, A. (2009) Three-dimensional structure and orientation of rat islet amyloid polypeptide protein in a membrane environment by solution NMR spectroscopy. *J. Am. Chem. Soc. 131*, 8252−8261.

(37) Brender, J. R., Salamekh, S., and Ramamoorthy, A. (2012) Membrane disruption and early events in the aggregation of the diabetes related peptide IAPP from a molecular perspective. *Acc. Chem. Res. 45*, 454−462.

(38) Williamson, M. P., Suzuki, Y., Bourne, N. T., and Asakura, T. (2006) Binding of amyloid β-peptide to ganglioside micelles is dependent on histidine-13. *Biochem. J. 397*, 483−490.

(39) Coles, M., Bicknell, W., Watson, A. A., Fairlie, D. P., and Craik, D. J. (1998) Solution structure of amyloid β-peptide(1−40) in a water−micelle environment. Is the membrane-spanning domain where we think it is? *Biochemistry 37*, 11064−11077.

(40) Shao, H., Jao, S.-C., Ma, K., and Zagorski, M. G. (1999) Solution structure of micelle-bound amyloid β-(1−40) and β-(1−42) peptides of Alzheimer's disease. *J. Mol. Biol. 285*, 755−773.

(41) Jarvet, J., Danielsson, J., Damberg, P., Oleszczuk, M., and Graslund, A. (2007) Positioning of the Alzheimer Aβ (1−40) peptide in SDS micelles using NMR and paramagnetic probes. *J. Biomol. NMR 39*, 63−72.
(42) Utsumi, M., Yamaguchi, Y., Sasakawa, H., Yamamoto, N., Yanagisawa, K., and Kato, K. (2008) Up-and-down topological mode of amyloid β-peptide lying on hydrophilic/hydrophobic interface of ganglioside clusters. *Glycoconjugate J. 26*, 999−1006.
(43) Wakabayashi, M., and Matsuzaki, K. (2007) Formation of amyloids by Aβ-(1−42) on NGF-differentiated PC12 cells: Roles of gangliosides and cholesterol. *J. Mol. Biol. 371*, 924−933.
(44) Klunk, W. E., Pettegrew, J. W., and Abraham, D. J. (1989) Quantitative evaluation of Congo red binding to amyloid-like proteins with a β-pleated sheet conformation. *J. Histochem. Cytochem. 37*, 1273−1281.
(45) Biancalana, M., and Koide, S. (2010) Molecular mechanism of Thioflavin-T binding to amyloid fibrils. *Biochim. Biophys. Acta 1804*, 1405−1412.
(46) Berthelot, K., Ta, H. P., Géan, J., Lecomte, S., and Cullin, C. (2011) In vivo and in vitro analyses of toxic mutants of HET-s: FTIR antiparallel signature correlates with amyloid toxicity. *J. Mol. Biol. 412*, 137−152.
(47) Stroud, J. C., Liu, C., Teng, P. K., and Eisenberg, D. (2012) Toxic fibrillar oligomers of amyloid-β have cross-β structure. *Proc. Natl. Acad. Sci. U.S.A. 109*, 7717−7722.
(48) Law, A., Gauthier, S., and Quirion, R. (2001) Say NO to Alzheimer's disease: The putative links between nitric oxide and dementia of the Alzheimer's type. *Brain Res. Rev. 35*, 73−96.
(49) Igbavboa, U., Avdulov, N. A., Schroeder, F., and Wood, W. G. (1996) Increasing age alters transbilayer fluidity and cholesterol asymmetry in synaptic plasma membranes in mice. *J. Neurochem. 66*, 1717−1725.
(50) Hayashi, H., Igbavboa, U., Hamanaka, H., Kobayashi, M., Fujita, S. C., Wood, W. G., and Yanagisawa, K. (2002) Cholesterol is increased in the exofacial leaflet of synaptic plasma membranes of human apolipoprotein E4 knock-in mice. *NeuroReport 13*, 383−386.
(51) Yamamoto, N., Matsubara, T., Sato, T., and Yanagisawa, K. (2008) Age-dependent high-density clustering of GM1 ganglioside at presynaptic neuritic terminals promotes amyloid β-protein fibrillogenesis. *Biochim. Biophys. Acta 1778*, 2717−2726.
(52) Bugiani, O., Giaccone, G., Verga, L., Pollo, B., Ghetti, B., Frangione, B., and Tagliavini, F. (1990) Alzheimer patients and Down patients: Abnormal presynaptic terminals are related to cerebral preamyloid deposits. *Neurosci. Lett. 119*, 56−59.
(53) Probst, A., Langui, D., Ipsen, S., Robakis, N., and Ulrich, J. (1991) Deposition of β/A4 protein along neuronal plasma membranes in diffuse senile plaques. *Acta Neuropathol. 83*, 21−29.
(54) Yamamoto, N., Hirabayashi, Y., Amari, M., Yamaguchi, H., Romanov, G., Van Nostrand, W. E., and Yanagisawa, K. (2005) Assembly of hereditary amyloid β-protein variants in the presence of favorable gangliosides. *FEBS Lett. 579*, 2185−2190.
(55) Yamamoto, N., Van Nostrand, W. E., and Yanagisawa, K. (2006) Further evidence of local ganglioside-dependent amyloid β-protein assembly in brain. *NeuroReport 17*, 1735−1737.
(56) Hayashi, H., Kimura, N., Yamaguchi, H., Hasegawa, K., Yokoseki, T., Shibata, M., Yamamoto, N., Michikawa, M., Yoshikawa, Y., Terao, K., Matsuzaki, K., Lemere, C. A., Selkoe, D. J., Naiki, H., and Yanagisawa, K. (2004) A seed for Alzheimer amyloid in the brain. *J. Neurosci. 24*, 4894−4902.
(57) Yamamoto, N., Yokoseki, T., Shibata, M., Yamaguchi, H., and Yanagisawa, K. (2005) Suppression of Aβ deposition in brain by peripheral administration of Fab fragments of anti-seed antibody. *Biochem. Biophys. Res. Commun. 335*, 45−47.